Humanoid Robot Motion Control for Ramps and Stairs

Tommy Truong

Alfredo Weitzenfeld

University of South Florida

ABSTRACT

Humanoid robot research and development have been an ongoing effort for many years. Tasks such as humanoid robot walking have been extensively researched, and can be often solved using control theory. In this paper, we explore how a Darwin-Op humanoid robot can autonomously balance and walk on non-flat terrains that include ramps and stairs. We use computer vision to detect the specific type of non-flat terrain based on color. Once the specific terrain has been identified, the humanoid robot computes the distance and orientation that it needs to walk before stopping. We developed the walking model using zero moment point (ZMP) trajectory planning with a cart-table model for the center of mass. We show that the robot is able to walk up the stairs and ramps, and compare experimental results with both stairs and ramps Keywords: Inverse Kinematics, Gait Planning, Computer Vision, Humanoid Robot

1. Introduction

As humanoid robots research advanced, the need for fluid human-like motions are needed such as grasping or walking. In the case of walking, we develop the need for humanoid robots to be able to move autonomously which can be done with the help of control theory, including gait planning. Gait planning is essentially a cyclic motion pattern to produce locomotion in legged robots [1]. To make humanoids more human-like, they must be able to walk under all sorts of conditions and terrains such as ramps or stairs.

Autonomous walking is an ability that humans do naturally without much intuition since we don't have to think about where we're going. Only in the instance where a person needs to take careful steps do we think about where to go. This problem translates directly to a humanoid robot because before it can walk autonomously, it needs to map out how and where it's going to walk. For a proof of concept work of showing how everything works, we explore how the Darwin-Op walks up a set of stairs and ramps using basic color detection for vision control, and Cart Table model and Zero Moment Point (ZMP) for the gait planning.

2. Kinematics

The kinematics calculated will be for the Darwin-Op and can be found based on the motor position on Figure 1 [2].Kinematics depends on the robot's measurements and limits. Since we are only concerned about the bipedal motion of the robot, we'll only look at the lower body of the robot. The the measurements and angle limits can be found on Table 1, 2, and 3 [3]. The left leg joint limits is inverse of the right leg, but the ankle limits are the same for both. For table 1, L_4 is the distance between motor 11 and 13, L_5 is the distance between motor 13 and 15, and L_F is the distance between motor 15 and the foot. In Table 2, F_X is the length of the foot, F_Y is the foot height, F_Z is the foot width, L_X is the length of the foot centered with the ankle joint front-to-back, and L_Z is the distance from the inner edge of the foot to the ankle joint.

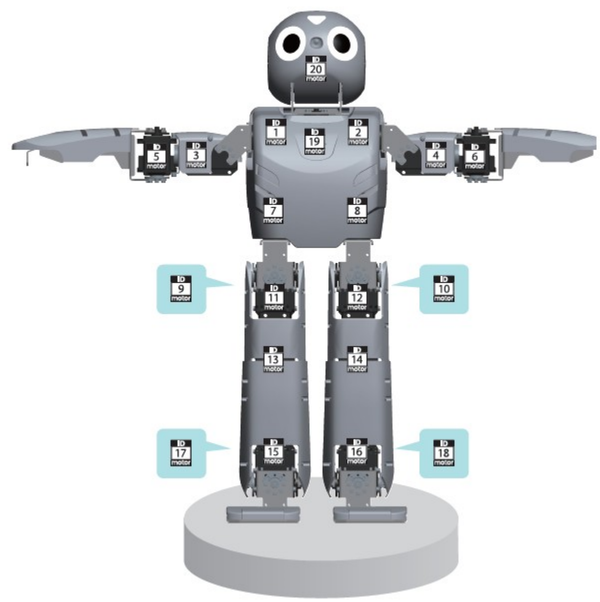

Figure 1. Darwin-Op Motor Positions

Length	Value (mm)
L_4	93.0
L_5	93.0
L_F	33.5

Table 1. Leg Lengths

Length	Value (mm)
F_X	104.0
F_Y	15.0 (10.0 front)
F_Z	66.0
L_X	52.0
L_Z	23.0

Table 2. Foot Lengths

Joint i	Joint name	Axis	Θ_{iMIN}	Θ_{iMAX}
1	Hip Yaw	Z_1	-150	45
2	Hip Roll	Z_2	0	60
3	Hip Pitch	Z_3	-100	30
4	Knee	Z_4	0	130
5	Ankle Pitch	Z_5	-60	60
6	Ankle Roll	Z_6	-30	60

Table 3. Right Leg Joint Limits

We will computed the kinematics using Denavit-Hartenburg (DH) parameters; DH parameters is a convection used to assign reference frames of a robot manipulator with respect to the x and z-axis. The leg has 6 degrees of freedom (DOF) with parameters described in Table 4; α_{i-1} is the angle between Z_i and Z_{i+1} along X_i, a_{i-1} is the distance between Z_i and Z_{i+1} along X_i, d_i is the distance between X_i and X_{i+1} along Z_i, θ_i is the angle between X_i and X_{i+1} along Z_i, i is the joint connecting link $i-1$ to link i. With the DH Table, the inverse kinematics can be found trivially using some numerical approaches in python.

i	α_{i-1}	a_{i-1}	d_i	Θ_i
1	0	0	0	θ_1
2	90	0	0	θ_2 + 90
3	90	0	0	θ_3
4	0	L_4	0	θ_4
5	0	L_5	0	θ_5
6	-90	0	0	θ_6

Table 4. Leg DH Parameters

3. Methodology

For the research, we simulated the work in Webots and assumed some general conditions for each environment. One obstacle per environment, no outside interference such as wind, floors would have friction to avoid slippage, and the noise level would be 0-10%.

With the assumption stated, the rest of this section will go over how autonomous locomotion is possible.

3.1 Vision Control

For the vision control, we went with a simpler approach of using known objects associated with a color. We went with this approach as it was easier to implement under the time constraint. When an object is detected, basic trigonometry is used to approximate the distance between the robot and the object. For the research we associated the following:

1. Start: Yellow
2. Goal: Green
3. Ramp: Gray
4. Stairs: Red

3.2 Gait Planning

For the gait planning, we used the cart-table model and ZMP [4]. The cart-table model describes the movement of the robot while ZMP describes the position of the supporting foot on the ground.

3.3 Zero Moment Point

Zero moment point was used because it determines if a biped robot is stable. It's considered stable when the total horizontal inertia and gravity forces equal 0 at a point on the ground [5]. This can be formalized in (eq) 1 where gi is the gravity plus inertia forces, m is the robot's mass, g is gravity, and a_G is the acceleration on the center of mass.

$$F^{gi} = mg - ma_G \tag{1}$$

Zero moment point is achieved when the moment around a point is parallel to the normal vector n as shown in (eq) 2. The moment (M_p) around a point (P) is shown in (eq) 3, and for the further explanation ZMP, the point used for ZMP will be shorten to Z as in (eq) 4; G is the center of mass, and H is the rate of angular momentum at the center of mass.

$$M_z^{gi} \times n = 0 \tag{2}$$

$$M_p = PG \times mg - PG \times ma_G - H_G \tag{3}$$

$$M_z^{gi} = ZG \times mg - ZG \times ma_G - H_G \tag{4}$$

From here, the Newton-Euler equation (eq) 5, and (eq) 6 can be used for the global motion of the biped robot; (eq) 5 is the resultant of the contact forces at point P, and (eq) 6 is the moment of the contact forces on point P. We set (eq) 5 to 0 to get (eq) 7 which then turns into (eq) 9. Similarly, setting (eq) 6 to 0 will result in (eq) 8 which then terns into (eq) 10. This process tells us that the biped robot is dynamically balanced if the contact forces (C) and the gravity inertia forces are strictly opposite as shown in (eq) 11; O is a point on the contact plane or the normal vector on G.

$$F^c + mg = ma_G \tag{5}$$

$$M_p^c + PG \times mg = H + PG \times ma_G \tag{6}$$

$$F^c + mg - ma_G = 0 \tag{7}$$

$$M_p^c + PG \times mg - H - PG \times ma_G = 0 \tag{8}$$

$$F^c + F^{gi} = 0 \tag{9}$$

$$M_p^c + M_p^{gi} = 0 \tag{10}$$

$$OZ = \frac{n \times M_O^{gi}}{F^{gi} \cdot n} \tag{11}$$

3.4 Cart-Table Model

The cart-table model was used because it simplifies the problem of describing in how to move the robot. The cart is assumed to be the upper-body of the robot and is located on the robot center of mass (CoM) where the mass is the total mass of the robot. The table is the supporting foot of the cart. We assumed two sets of cart-table to described the movement in the coronal and sagittal plane. The coronal plane is shown in 2 which divides the body in the half from front to back and the sagittal plane is shown in 3 which divides the body in half from left to right.

To determine the ZMP for the cart-table model on Figure 2, we set the cart position in the coronal plane to be at x and Z_h; Alternatively for the sagittal plane, the cart position is at y and Z_h The moment T_p or amount of torque around a point is represented as the red point; This point also represents the center of pressure (CoP) as

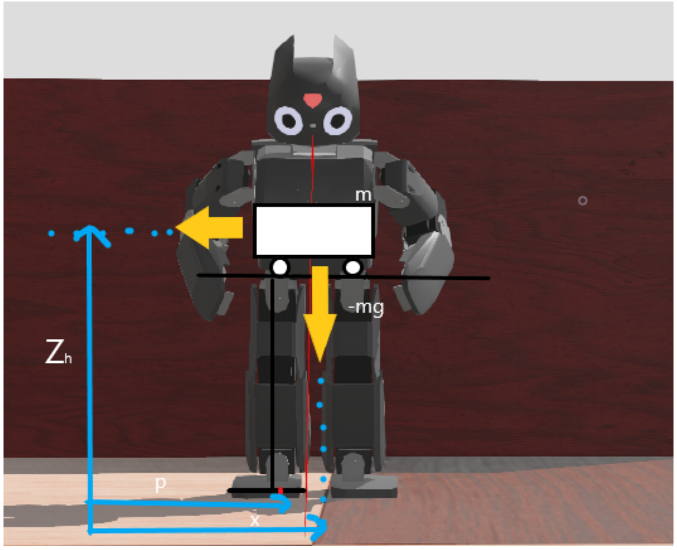

Figure 2. Coronal View of the Cart-Table Model

Figure 3. Sagittal View of the Cart-Table Model

gravity g and the cart accelerate. This process for the coronal plane is shown in (eq) 12. The same logic applies for the sagittal plane but instead of x, it's y in (eq) 13. $\ddot{x}$ and $\ddot{y}$ represents the acceleration of the center of mass in the coronal and sagittal plane respectively.

$$M_x = mg(x - P_x) - m\ddot{x}Z_h \tag{12}$$

$$M_y = mg(y - P_y) - m\ddot{y}Z_h \tag{13}$$

In the balanced robot, the ZMP and CoP have to be identical meaning the moment is 0 or $T_p = 0$. By setting the left hand side of (eq) 14 to 0, (eq) 15 can be achieved which then we can solve for the position for the ZMP as seen in (eq) 16 and (eq) 17. Therefore, the positioning of the foot during walking is defined with those constraints.

$$0 = Mg(x - P_x) - m\ddot{x}Z_h \tag{14}$$

$$m\ddot{x}Z_h = mg(x - P_x) \tag{15}$$

$$P_x = x - \frac{Z_h}{g}\ddot{x} \tag{16}$$

$$P_y = y - \frac{Z_h}{g}\ddot{y} \tag{17}$$

3.5 Trajectory Planning

To further generalize how the gaits needs to be plane, we path plan where the foot has to go. Following Figure 4, if we know the constraints of the stairs such as step height and step width then we can plan a gait cycle that has a leg swing that goes H_s high and X_s far. The trajectory planning for ramp is simpler because the gait cycle would remain constant since the only thing that changes is the orientation of the foot; orientation of the foot would be the incline angle of the ramp.

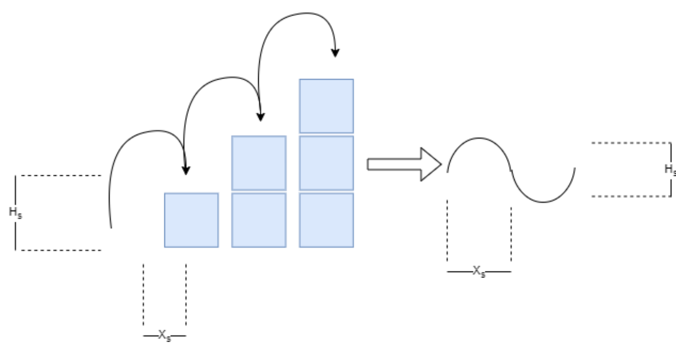

Figure 4. Stair Trajectory Planning

4. Simulation

For the simulation, we used Webots as it was a robot simulator that already had the Darwin-Op model. The drawback is that the model can't be modified such as grippers but extra sensors can still be attach to the model. With the simulation, we were able to create 2 environments to test the robot, a stair set as seen on Figure 5 and a ramp set as seen on Figure 6. For the programming, we used Python 3.8 to help with the numerical calculations and computer vision. We used OpenCV for the color detection and NumPy for the math calculations.

5. Experiment

For the research conducted, we tested the performance of the control system by changing the parameters on the obstacle and on the robot. Below shows the parameters changed for performance analysis.

- Robot: Speed
- Ramp: Angle

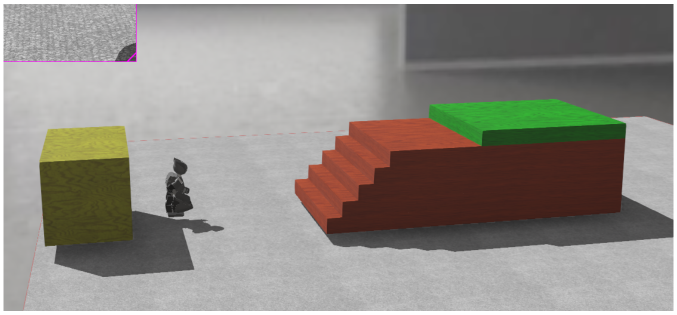

Figure 5. Stair Environment

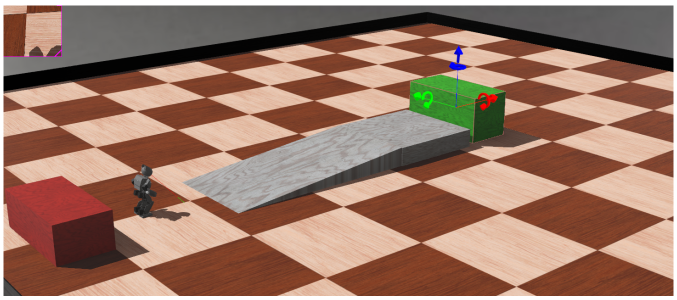

Figure 6. Ramp Environment

- Stairs: Step Height

For the speed parameter, we setup 3 different speeds (slow, normal, fast), for the experiment, we considered speed to be the length of time needed to complete one step. Normal is the base rate it took to finish one successful trial, while the slow and fast speeds are 2x slower and faster than the base rate respectively. The result of each experiment can be found in Section 5.1 and 5.2. Each trail had 10 runs with the speeds changing for each trial; A successful run occurred when the robot was able to walk the obstacle course without falling.

5.1 Ramp Experiment

According to the Americans with Disabilities Act (ADA) standard, the maximum ramp slope is 18 degrees[6]. Therefore, the ramp experiment is to see what the maximum incline the robot can handle and if it's the same as a human. While 18 is the maximum ramp slope, the steepest angle a human can climb is 30 degrees. Therefore the setup of the ramp experiment is the minimum incline of 2 degrees, and 30 degrees for the maximum with 4 degrees increment with each trial.

5.2 Stair Experiment

According to Florida's Building Codes, the residential stairway riser must be at least 4 inches with a maximum of 7.75 inches[7]; The riser height is determined relative to a human ankle height. The riser height is also the height where humans can walk without external support which is the test purpose for the Darwin-Op. For the stair experiment, a modification to the minimum and maximum height is needed since Darwin-Op's lower leg is only 3.66 inches and the ankle height 1.32 inches. Since a normal stairway is larger than what the robot can handle, the stairs were scaled down proportional to what the robot can handle. For the new scaled down stairs, the minimum riser height would be .5 inches with the maximum being 1.5 inches. We test these two range with a .3 inch increment for each trial.

6. Results

The results of both experiments are described in Section 6.1 and 6.2. A "pass" indicated that all runs in a trial were successful. A "fail" indicated that it failed all runs in a trial, and "x/10" indicates the amount of runs passed in a trial.

6.1 Ramp Results

For the results shown in Table 5, it successfully passed all trials up to an incline of 14 degrees. Some failures can be seen on the 18-degree mark which were due to slippage on fast speeds. While it was expected, it was shown that the robot could not handle a steep 30-degrees incline. The issues with the 30 degree incline is getting a stable footing, most of the failures were from slipping in the first step on the incline.

Angle (degrees)	Slow	Normal	Fast
2	pass	pass	pass
6	pass	pass	pass
10	pass	pass	pass
14	pass	pass	pass
18	pass	pass	7/10
30	fail	fail	fail

Table 5. Ramp Experiment

6.2 Stair Results

For the results shown in Table 6, there were more inconsistencies shown as the step height of .7 inches had better results than a step height of .5. Overall, no trial had a complete success, and the trials with steps height higher than 1.1 quickly worsen. Some explanations for this is the robot failing to step high enough to completely go to the next step. If it was a little off over or under, it caused the robot to hit the edge of the step thus failing down.

Step Height (inch)	Slow	Normal	Fast
0.5	4/10	4/10	4/10
0.7	5/10	5/10	3/10
0.9	3/10	3/10	1/10
1.1	2/10	2/10	1/10
1.3	fail	fail	fail
1.5	fail	fail	fail

Table 6. Stairs Experiment

6.3 Model Summary

7. Conclusions

The paper described how Darwin-Op can autonomously travel non-flat terrains. By using a cart-table model for the ZMP trajectory planning, the robot was able to plan path for keeping itself balanced. We can conclude that ramps are the easiest to walk on, while stairs leave room for more improvement.

Parameter	Definition
L_4	Distance between motor 11 and 13
L_5	Distance between motor 13 and 15
L_F	Distance between motor 15 and foot
F_X	Length of the foot
F_Y	Width of the foot
F_Z	Height of the foot
L_X	Length of the foot centered with the ankle joint
L_Z	Distance from inner edge of the foot to ankle joint

Table 7. Parameter Table

Variable	Definition
i	Joint connecting link $i-1$ and link i
Θ_i	Angle between X_i and X_{i+1} along Z_i
α_{i-1}	Angle between Z_i and Z_{i+1} along X_i
d_i	Distance between X_i and X_{i+1} along Z_i
F	Force
gi	Gravity inertia
m	robot mass
g	Gravity
a	acceleration
G	Center of Mass
P	Point of consideration
M_P	Moment at a point
M_z	Moment at the ZMP point
M_x	Moment around x
M_y	Moment around y
Z	ZMP point
H	Rate of angular momentum
C	Contact forces
n	Normal vector
O	Point on contact plane
x	Cart position in coronal plane
$\ddot{x}$	Cart acceleration in coronal plane
P_x	ZMP for coronal plane
y	Cart position in sagittal plane
$\ddot{y}$	Cart acceleartion in sagittal plane
P_y	ZMP for sagittal plane
Z_h	Cart height position

Table 8. Variable Table

8. Future Work

For areas of improvement, we could refine the walking process for the stair climbing. Instead of pre-planning the steps, it could switch to a more reactive approach to handle one step at a time. For the vision control, it can be updated to an object detection based model to be able to recognized more terrains and make the system more robust.

Initially the research proposed was intended for ladder climbing, but because of the limitation of the simulation software, it was not accomplished [8]. The next step in this research would be to either use a new simulation software or model the robot with new grippers.

Acknowledgement

This work was funded in part by NSF IIS Robust Intelligence research collaboration grant #1703225 at the University of South Florida entitled "Experimental and Robotics Investigations of Multi-Scale Spatial Memory Consolidation in Complex Environments".

References

[1] G. C. Haynes and A. A. Rizzi, "Gaits and gait transitions for legged robots," *2006 IEEE International Conference on Robotics and Automation*, May 2006.

[2] Cyberbotics, "Webots: robot simulator." `https://cyberbotics.com/`, 1998.

[3] R. L. Williams, "Darwin-op humanoid robot kinematics," *IDETC/CIE 2012*, August 2012.

[4] Y.-L. Hwang, T.-N. Ta, C.-H. Chen, and K.-N. Chen, "Using zero moment point preview control formulation to generate nonlinear trajectories of walking patterns on humanoid robots," in *2015 12th International Conference on Fuzzy Systems and Knowledge Discovery (FSKD)*, pp. 2405–2411, 2015.

[5] P. Sardain and G. Bessonnet, "Forces acting on a biped robot. center of pressure - zero moment point," *IEEE Transactions On Systems, Man, and Cybernetics - Part A: Systems and Humans*, September 2004.

[6] A. with Disabilities Act, "Building access ramp slope or pitch requirements." `https://inspectapedia.com/Stairs/Access_Ramp_Slope`.

[7] R. Cooks, "Florida building codes for residential stairs." `https://www.hunker.com/13402630/florida-building-codes-for-residential-stairs`.

[8] I. Ha, Y. Tamura, and H. Asama, "Development of open platform humanoid robot darwin-op," *Advanced Robotics*, vol. 27, pp. 223–232, January 2012.